Letter

Ultrastrongly coupled and directionally nonreciprocal magnon polaritons in magnetochiral metamolecules

Kentaro Mita,[1] Takahiro Chiba,[2,3] Toshiyuki Kodama,[4] Tetsuya Ueda,[5] Toshihiro Nakanishi,[6] Kei Sawada,[7] and Satoshi Tomita[1,4,*]

[1] *Department of Physics, Graduate School of Science, Tohoku University, Sendai 980-8578, Japan*
[2] *Frontier Research Institute for Interdisciplinary Sciences, Tohoku University, Sendai 980-8578, Japan*
[3] *Department of Applied Physics, Graduate School of Engineering, Tohoku University, Sendai 980-8579, Japan*
[4] *Institute for Excellence in Higher Education, Tohoku University, Sendai 980-8576, Japan*
[5] *Department of Electrical Engineering and Electronics, Kyoto Institute of Technology, Kyoto 606-8585, Japan*
[6] *Department of Electronic Science and Engineering, Kyoto University, Kyoto 615-8510, Japan*
[7] *RIKEN SPring-8 Center, Sayo 679-5148, Japan*

(Received 29 July 2024; revised 18 December 2024; accepted 20 December 2024; published 17 January 2025)

We experimentally demonstrate magnon polaritons with ultrastrong coupling and directional nonreciprocity in a metamolecule lacking time-reversal and space-inversion symmetries at room temperature. These experimental results are reproduced well via numerical simulations and theoretical considerations. Ultrastrong coupling is due to a direct interaction of magnons in the magnetic meta-atom with microwave photons confined in the chiral meta-atom as a resonator. Our results reveal a crucial step in identifying deep strongly coupled and optically moving magnon polaritons for hybrid quantum systems, synthetic gauge fields, and quasiparticle "chemistry" using metamaterials.

DOI: 10.1103/PhysRevApplied.23.L011004

Introduction. Condensed matter physics is a field of various quasiparticles with elementary excitations. Integrating different quasiparticles has led to novel and intriguing properties of matter and opened up an essential pathway toward frontiers in physics [1,2]. A magnon, a quantized elementary excitation in magnets, can be transformed to a magnon polariton (MP) when it is coupled to alternating current (ac) electromagnetic fields, namely photons. The MP has gained attention particularly in quantum information technology and spintronics [3,4] for applications to hybrid quantum systems [5].

Magnons and photons are coherently coupled—strong coupling—if the coupling constant, g, is larger than the dissipation rate, κ, in a resonator and oscillator ($g > \kappa$), generating MP. Here, g is given by $g = (\omega_+ - \omega_-)/2$, where $\omega_\pm$ are the hybridized eigenmodes at the crossing point of the original modes. Such coherent coupling of magnons with photons having a frequency of $\omega/2\pi$ gives rise to the dispersion anticrossing due to the hybridization. The anticrossing is evaluated using Rabi-like level repulsion of $2g/2\pi$, which is proportional to a coupling ratio of g/ω. While the strong coupling is characterized by $g > \kappa$, an ultrastrong magnon-photon coupling is represented by $g > \kappa$ and $g/\omega > 0.1$, which is indispensable toward the quantum regime [6]. The ultrastrongly coupled MPs have been demonstrated at microwave frequencies using magnetic heterostructures composed of superconductors [7–9]. They are, however, operated at cryogenic temperatures. Therefore, operating ultrastrongly coupled MPs at room temperature remains challenging.

The ultrastrongly coupled MP is inherently nonreciprocal owing to the breaking of time-reversal symmetry by magnetization or magnetic fields [10]. With the additional breaking of the space-inversion symmetry, the nonreciprocity results in a transmission amplitude (and phase) difference depending on the propagation direction of photons. However, such a directionally nonreciprocal optical phenomenon has yet to be observed in ultrastrongly coupled systems, except for dissipative [11] or strong [12] magnon-photon coupling. The directionally nonreciprocal phenomena exist in natural chiral molecules [13–15], multiferroic materials [16], and metamaterials [17–19] under external direct current (dc) magnetic fields, as polarization-independent phenomena—magnetochiral (MCh) and optical magnetoelectric (ME) effects [20,21]. Although such nonreciprocal MCh metamaterials indicate the presence of room-temperature coherent couplings between magnons and photons at microwave frequencies [18], the coupling mechanism remains unclear. The coupling mechanism should therefore be clarified by evaluating the coupling ratios of the MP.

In this letter, we demonstrate experimentally and numerically ultrastrong couplings of the directionally

*Contact author: tomita@tohoku.ac.jp

nonreciprocal MPs in a single three-dimensional MCh metamolecule at room temperature. The coupling ratio is evaluated to be $g/\omega > 0.2$, which is achieved by direct interaction between magnons in the yttrium iron garnet (YIG) cylinder and microwave photons in the Cu chiral structure as a resonator. Further enhancement of the coupling ratio can be achieved by a decrease in the frequency of the fundamental mode of the chiral resonance, bringing about the deep strong coupling for hybrid quantum systems. Moreover, the metamolecule including the chiral resonator paves the way to directionally nonreciprocal MPs in free space for synthetic gauge fields for photons. Furthermore, the synthesis of metamolecules and metamaterials by combining different meta-atoms leads to quasiparticle "chemistry."

Experimental setup. Figure 1(a) is an illustration of the MCh metamolecule. The MCh metamolecule consists of a polycrystalline YIG cylinder (as a magnetic meta-atom) inserted in a right-handed helix made of copper (Cu) (as a chiral meta-atom) [18]. The Cu wire of 0.55-mm diameter is wound four times with a 2.6-mm pitch to form a right-handed helix of 2.55-mm outer diameter. The YIG cylinder is 2 mm in diameter and 15 mm in length.

As in Fig. 1(b), the MCh metamolecule is set into a WR-90 waveguide that supports the TE_{10} mode with square flange adapters (Pasternack PE9804). The metamolecule is oriented to the x axis, which is parallel to the ac magnetic field in the WR-90 waveguide. See Fig. S1 in the Supplemental Material [22] for the ac magnetic and electric fields of the TE_{10} mode in the waveguide. An external dc magnetic field, $\mu_0 H_{\text{ext}}$, up to approximately 540 mT is applied in the $+z$ direction by an electromagnet. The waveguide is connected to a vector network analyzer (VNA; Rohde & Schwarz ZVA67) with a microwave input power of 0 dBm (1 mW). The S parameters are measured using the VNA. The S_{21} indicates a complex transmission coefficient from port 1 to 2, while S_{12} represents that from port 2 to 1. All measurements are carried out at room temperature.

Experimental results. Figure 1(c) illustrates the transmission amplitude $|S_{21}|$ spectra of the x-axis-oriented MCh metamolecule from 7 to 14 GHz under varying $\mu_0 H_{\text{ext}}$ (0–543 mT). Without the dc magnetic field ($\mu_0 H_{\text{ext}} = 0$), two sharp dips are observed: one at 9.34 GHz (A) and the other at 12.36 GHz (B). Based on numerical simulation using COMSOL Multiphysics of the metamolecule under $\mu_0 H_{\text{ext}} = 0$, we confirm that the dip at the lower frequency is caused by the third-order resonance, with two nodes in the Cu chiral meta-atom induced by the microwave photons with the ac magnetic field in the x axis (see Fig. S2(a) and Movie S1 in the Supplemental Material [22]). The dip A at 9.34 GHz is thus traced back to the resonating photons, referred to as chiral resonant photons, because the chiral meta-atom functions as a resonator or sensitizer. Contrastingly, the dip B at higher frequency is caused

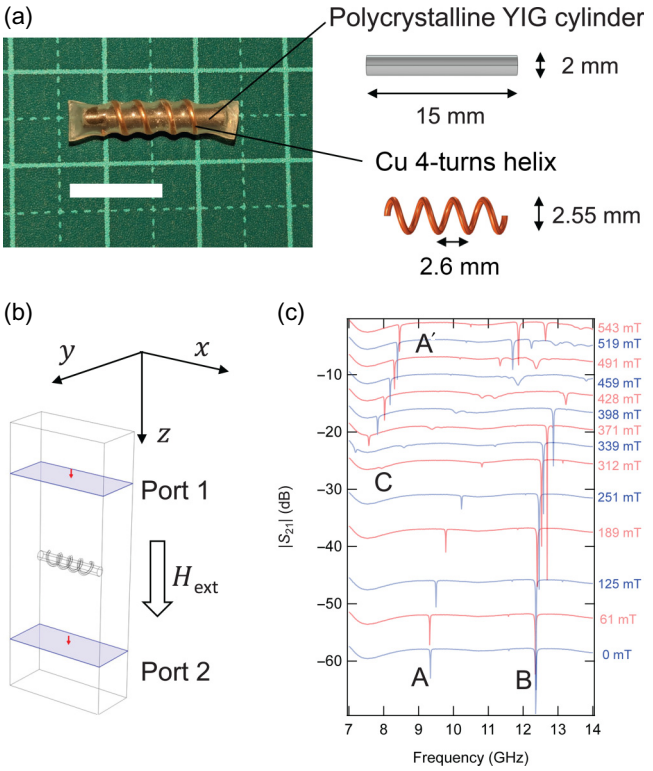

FIG. 1. Magnetochiral (MCh) metamolecule under study, measurement setup, and measured microwave spectra of the metamolecule. (a) Sample photo and constituents. The white scale bar corresponds to 10 mm. (b) Measurement and simulation setup of the x-axis-oriented metamolecule placed in a waveguide. (c) The $|S_{21}|$ amplitude spectra of the x-axis-oriented metamolecule at various magnetic fields.

not by simple resonance but by a complex mode with tornado-like current distribution in the Cu chiral structure or Mie resonance by the displaced YIG cylinder (see Figs. S2(a) and S2(c) and Movie S2 in the Supplemental Material [22]). Therefore, in this experiment, we focus on the third-order chiral resonant photon at approximately 9 GHz, which is labeled as A.

Applying the external dc magnetic field to the metamolecule in the $+z$ direction causes the chiral resonant photon mode A to shift slightly to a lower frequency at $\mu_0 H_{\text{ext}} = 61$ mT and then turn to a higher frequency with increasing $\mu_0 H_{\text{ext}}$. The major blue shift of the chiral resonant photon mode is attributed to the magnetic permeability change of the YIG cylinder by the applied $\mu_0 H_{\text{ext}}$, which is evidence of the interaction between the YIG magnetic meta-atom and the microwave photon in the Cu chiral meta-atom. When $\mu_0 H_{\text{ext}} = 312$ mT, a slight dip appears at approximately 8 GHz labeled as C in Fig. 1(c). The slight dip keeps moving to a higher frequency with increase in $\mu_0 H_{\text{ext}}$ up to 543 mT; therefore, the dip is caused by ferromagnetic resonance, i.e., a magnon, in the YIG magnetic meta-atom. When $\mu_0 H_{\text{ext}} = 339$ mT, the magnon mode C approaches the chiral resonant photon

mode A. Simultaneously, another sharp dip appears at 7.19 GHz, denoted by A′, and shifts to a higher frequency with a further increase in $\mu_0 H_{\text{ext}}$. This indicates the hybridization of chiral resonant photon modes A and A′ with the magnon mode C, demonstrating the coherent coupling between chiral resonant photons and magnons in the metamolecule.

In Fig. 2(a), $|S_{21}|$ is plotted two-dimensionally as a function of $\mu_0 H_{\text{ext}}$ from 0 to 543 mT (horizontal axis) and of frequency from 7 to 14 GHz (vertical axis) to evaluate the magnon-photon coupling strength. The black color corresponds to a higher transmission in the $|S_{21}|$ spectra, while the yellow to white colors correspond to lower transmissions. Green dotted lines correspond to guides for the eye of the chiral resonant photon frequency and the magnon mode. The $|S_{21}|$ two-dimensional (2D) plot in Fig. 2(a) highlights, at $\mu_0 H_{\text{ext}} \sim 350$ mT, the anticrossing between the chiral resonant photon mode A with $\omega_a/2\pi = 9.34$ GHz and the magnon mode C. The anticrossing Rabi-like level splitting of chiral resonant photon modes A and A′ is $g/\pi = 4.19$ GHz at $\mu_0 H_{\text{ext}} = 367.7$ mT, resulting in a coupling ratio of $g/\omega_a = 0.22$. The coupling ratio g/ω_a larger than 0.1 demonstrates that magnons in the YIG cylinder and photons in the Cu chiral structure in the MCh metamolecule are ultrastrongly coupled at room temperature. The coupling ratio can be varied by the metamolecule orientation. Figures S3(a), S3(b), and S3(c) in the Supplemental Material [22] indicate that the z-axis-oriented metamolecule has a smaller coupling. The coupling ratio is thus relevant to the electromagnetic mode.

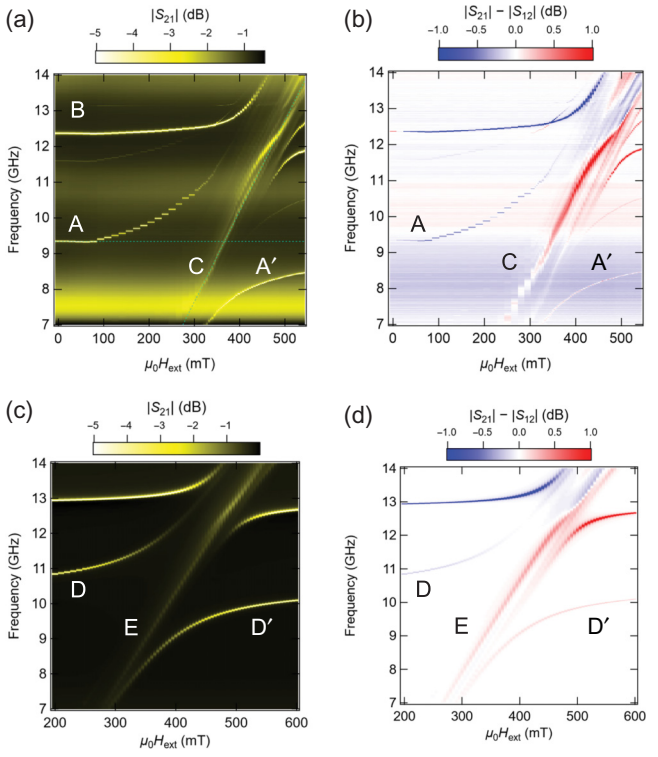

FIG. 2. Two-dimensional plot of measured and simulated MP dispersion. (a),(b) Measured 2D plots of (a) transmission amplitude $|S_{21}|$ and (b) amplitude difference $|S_{21}| - |S_{12}|$ of the x-axis-oriented metamolecule as functions of applied external dc magnetic field, $\mu_0 H_{\text{ext}}$, and frequency. (c),(d) Numerically simulated 2D plots, using COMSOL Multiphysics, corresponding to (a) and (b), respectively.

Figures S4(a) and S4(b) in the Supplemental Material [22] present the directional transmission amplitude difference, $|S_{21}| - |S_{12}|$, and phase difference, $\arg S_{21} - \arg S_{12}$, spectra of the MCh metamolecule in the x-axis orientation, respectively. We note that $|S_{21}| - |S_{12}|$ at approximately 12 GHz is larger than those of signals A and A′ at approximately 9 GHz. However, as mentioned above, the origin of the signal at approximately 12 GHz is ill-defined. Therefore, we focus on the well-defined signals A and A′ of the third-order chiral resonant photon. Using Fig. S4(a), a 2D plot of experimentally observed $|S_{21}| - |S_{12}|$ is drawn in Fig. 2(b). The red color corresponds to $|S_{21}| > |S_{12}|$, while the blue color corresponds to $|S_{21}| < |S_{12}|$. The chiral resonant photon mode A above the magnon mode line C demonstrates $|S_{21}| < |S_{12}|$, while the mode A′ below the magnon mode C represents $|S_{21}| > |S_{12}|$. This is characteristic of the directional nonreciprocity of ultrastrongly coupled MPs.

Numerical simulation. Simultaneous breaking of time-reversal and space-inversion symmetries by the coexistence of magnetism and chirality in the metamolecule is the primary origin of the directional nonreciprocity observed in Fig. 2(b). An alternative and artificial origin could be a slight displacement of the metamolecule from the waveguide center or a misalignment of the metamolecule from the x axis because similar nonreciprocal signals have been observed by an asymmetrical microstrip line on a ferrite substrate [23] and a displaced magnetic material on a coplanar waveguide [24]. Indeed, in this study, numerical simulation indicates that the dip B observed at a higher frequency is caused by the Mie resonance of the displaced YIG cylinder. Therefore, we conduct numerical simulation of the metamolecule under various magnetic fields using COMSOL Multiphysics to exclude such an artificial origin. The Supplemental Material [22] details the numerical simulation method (see also Ref. [25] therein).

Figure 2(c) presents the numerically simulated 2D plot of $|S_{21}|$ as a function of $\mu_0 H_{\text{ext}}$ from 200 to 600 mT (horizontal axis) and of frequency from 7 to 14 GHz (vertical axis). Level repulsion due to the interaction between chiral resonant photons (D and D′) and magnons (E) is reproduced. The simulated coupling ratio of 0.15 derived from the level splitting of 3.21 GHz at $\mu_0 H_{\text{ext}} = 410$ mT is smaller than that observed experimentally in Fig. 2(a) because the magnetization dynamics in the YIG cylinder is linearized in the numerical simulation. Nevertheless, the simulated 2D plot of $|S_{21}| - |S_{12}|$ in Fig. 2(d) has successfully reproduced the directional nonreciprocity of the

MPs. The metamolecule has negligible dissipation and is regarded as a Hermitian system. As shown in Fig. 2(d), removal of the misalignment and displacement of the metamolecule in the simulation verifies that the origin of directionally nonreciprocal signals is the MP under the simultaneous breaking of time-reversal and space-inversion symmetries in the metamolecule.

Theoretical considerations. The coupling ratio of the MP is quantitatively reproduced by considering the magnetization dynamics. The experimental system is the forced oscillation of MPs driven by the input microwaves; nonetheless, a simpler damped oscillation model is assumed to reproduce the coupling ratio of the magnon and chiral resonant photons in the following. As in Fig. 3(a), $h_{n,x}$ represents an ac magnetic field in the x direction due to Ampère's circuit law accompanied by Faraday electromagnetic induction in the chiral meta-atom—chiral resonant photons. Here, the integer n denotes the mode index of the chiral resonant photons. The ac magnetic field $h_{n,x}$ excites magnons (m_x) in the YIG cylinder. This leads to direct coupling between magnons and chiral resonant photons, generating ultrastrongly coupled MPs in the metamolecule. Recall that the numerical simulation using COMSOL indicates that the third-order resonance with $n = 3$ ($h_{3,x}$) appears at approximately 10 GHz. Thus, the MPs can be described as a coupled oscillator model that considers a uniform magnon mode and two chiral resonant modes with $n = 3$ and 5. The Supplemental Material [22] presents the calculation details (see also Ref. [26] therein).

Figures 3(b) and 3(c) are calculated damped oscillations of the chiral resonant photons ($h_{n,x}$) and the magnons (m_x) under $\mu_0 H_{\text{ext}} = 0.39$ T for $n = 3$ and under $\mu_0 H_{\text{ext}} = 0.50$ T for $n = 5$, respectively. We assume the higher-frequency mode to be the fifth-order resonance. The time evolutions in Figs. 3(b) and 3(c) correspond to Rabi-like oscillations—the amplitude exchange between one chiral resonant photon (red or green) and a magnon (blue). A minimal complexity in the Rabi-like oscillations is attributed to interactions among three modes (one magnon and two chiral resonant photons) in the metamolecule.

Figures 3(d) and 3(e) correspond to the Fourier spectra of the time evolutions, in which three peaks represent coupled modes among one magnon and two chiral resonant photons, i.e., MP modes with Rabi-like frequency splitting. According to these spectra, the evaluated couplings are $g_3/\pi = 3.75$ and $g_5/\pi = 3.93$ GHz, resulting in coupling ratios of $g_3/\omega_3 = 0.20$ and $g_5/\omega_5 = 0.16$, respectively. Here, the subscripts in g_n and ω_n mean the corresponding values of the nth order. Based on the experimental results, $\omega_3/2\pi = 9.34$ and $\omega_5/2\pi = 12.36$ GHz are assumed for this evaluation. The computed $g_3/\omega_3 = 0.20$ is consistent with the experimentally obtained $g/\omega_a = 0.22$, indicating that MP in the MCh metamolecule is in the ultrastrong coupling regime. Moreover, $g_3/\omega_3 = 0.20$ and $g_5/\omega_5 = 0.16$ indicate that the coupling at a lower frequency is much stronger than that at a higher frequency.

Discussion. This study reveals that the MCh metamolecule consisting of a YIG cylinder inserted in a Cu chiral structure results in ultrastrongly coupled and directionally nonreciprocal MP at room temperature. Table S1 in the Supplemental Material [22] compares the temperature, MP coupling ratio, and nonreciprocity obtained in this study with those reported in the literature (see also Refs. [27,28] therein). Ultrastrong coupling in the MP is primarily caused by direct interaction between photons in the Cu chiral structure and magnons in the magnetic YIG cylinder via ac magnetic fields in the x direction. The coupling ratio is reduced in the z-axis-oriented metamolecule [see Fig. S3(c)] because electromagnetically induced ac magnetic fields in the z direction cannot drive magnons

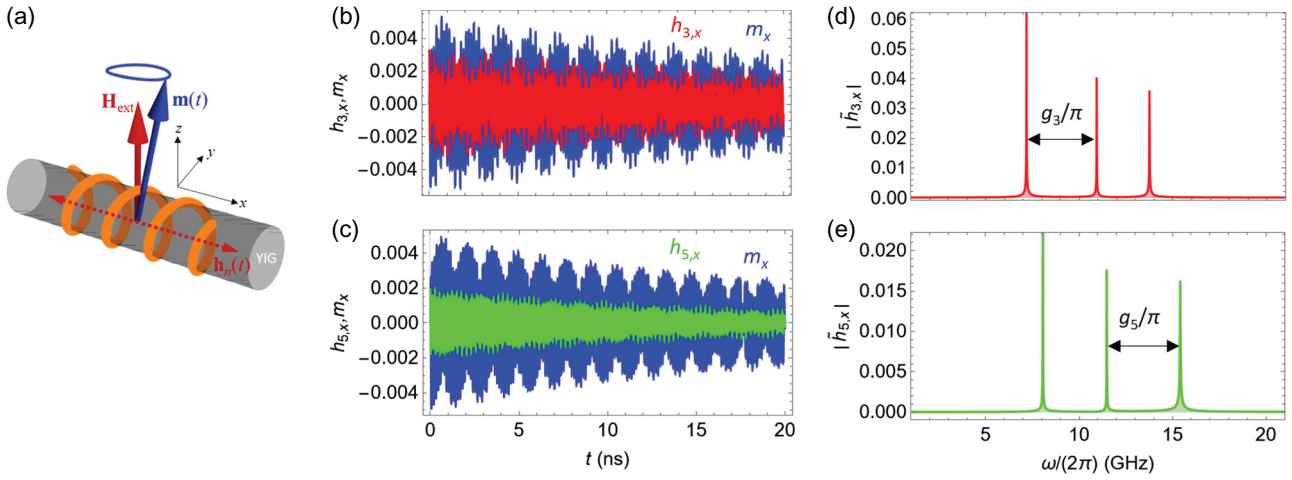

FIG. 3. Theoretical consideration including magnetization dynamics. (a) Schematic of MCh metamolecule composed of a Cu chiral structure involving a YIG cylinder. The metamolecule's YIG cylinder is oriented to the x axis. (b),(c) Rabi-like oscillations of the chiral resonant photons ($h_{n,x}$) and magnon (m_x) under (b) $\mu_0 H_{\text{ext}} = 0.39$ T ($n = 3$) and (c) $\mu_0 H_{\text{ext}} = 0.50$ T ($n = 5$), respectively. (d),(e) Corresponding Fourier spectra of chiral resonant photons ($h_{n,x}$) for (d) 9.34 GHz and (e) 12.36 GHz, respectively.

under the external dc magnetic field, $\mu_0 H_{\text{ext}}$, in the z direction. This results in indirect coupling between the chiral resonant photon and magnon in the z-axis-oriented metamolecule. Therefore, the coupling ratio can be enhanced by finding a suitable metamolecule orientation.

Utilizing the fundamental mode ($n = 1$) is another strategy toward achieving a much stronger coupling between magnons and photons—the deep strongly coupled MP, i.e., $g/\omega_a \geq 1$, in the metamolecule. In this experiment we use the third-order mode ($n = 3$) of the chiral resonant photon to obtain the highest value of $g/\omega_a = 0.22$; the magnon-photon coupling is thus reduced by $\eta_3 = 1/3$, where η_n is a phenomenologically introduced mode-dependent coefficient responsible for the space dependence of the microwave magnetic field in the MCh metamolecule. Here, we assume the net magnitude of the ac magnetic field of the chiral resonant photon to be inversely proportional to the number of antinodes (for more detail see the Supplemental Material [22]). In this way, the $n = 1$ fundamental mode may enhance the magnon-photon coupling by maximizing the electromagnetic induction due to the magnon dynamics.

Additionally, according to the theoretical prediction for the metamolecule [29], the coupling ratio is evaluated via $g/\omega_a \propto 1/\sqrt{\omega_a}$. Therefore, further enhancement toward the deep strong coupling is possible by decreasing the chiral resonant frequency, ω_a, of the fundamental mode by increasing the system size and changing the design of the metamolecule and materials of the constitutive meta-atoms. This enhancement in the coupling is attributed to increasing the total number of spins in the magnetic meta-atom. The deep strongly coupled MP will lead to mysterious quantum effects, such as vacuum Bloch-Siegert shift [30] and quantum squeezing under thermal equilibrium [31]. The Hermitian, ultrastrongly coupled, and directionally nonreciprocal MP may give rise to coherent quantum rectification of quantum information.

The second origin of the ultrastrong coupling in this study is the photon confinement in the chiral meta-atom. The chiral meta-atom functions as a resonator or sensitizer. Because the resonator is embedded in a metamolecule that supports MPs, the metamolecule may realize the MPs for propagating microwaves in free space. Indeed, as shown in Fig. S5 in the Supplemental Material [22], our additional numerical simulation using COMSOL verifies the free-space MP with ultrastrong coupling and directional nonreciprocity. The MP in free space is a central topic in quantum optics, as it allows control over individual quantum systems [32,33]. Moreover, the nonreciprocal MP in free space leads to the observation of polarization-independent optically moving effects. The optically moving effect in MCh and ME media exhibits an electromagnetic response equivalent to that of a regular material moving at relativistic speed [34–36]. Therefore, free-space MPs with ultrastrong coupling and directional nonreciprocity enable us to realize synthetic gauge fields, i.e., the Lorentz force acting on propagating microwaves [37].

Last but not least, the quasiparticle integration is comprehensively classified according to the interaction between polarization P and magnetization M. The conventional ME and MCh effects observed in this study are given by the coupling between P and M. In contrast, the dynamic coupling of the time derivatives of P and M results in a new collective mode corresponding to an MCh electromagnon polariton, which is still unclear but anticipated to be observed using metamaterials. Furthermore, we focus on magnons in this study; however, other quasiparticles, such as excitons, phonons, and plasmons, can be integrated in metamaterials. Thus, this study signifies a pivotal advancement toward expounding quasiparticle "chemistry" using metamaterials.

Conclusion. We demonstrate ultrastrong coupling of the directionally nonreciprocal MPs in a single MCh metamolecule at room temperature. The metamolecule exhibits the coupling ratio of $g/\omega = 0.22$, which is achieved by direct interaction between magnons in the YIG meta-atom and microwave photons confined in the Cu chiral meta-atom as the resonator. These experimental results are reproduced well via numerical simulations and theoretical considerations. The coupling ratio and directional nonreciprocity can be enhanced by changing the metamolecule orientation and the chiral resonance frequency. The MCh metamolecule represents a crucial step toward developing hybrid quantum systems and quasiparticle "chemistry" using metamaterials. Furthermore, optically moving MPs by metamolecules in free space enable us to realize the Lorentz force acting on propagating microwaves.

Acknowledgments. We thank H. Yasuda and Y. Motoda for their technical support with the microwave measurements and H. Kurosawa for helping with the numerical simulation. This work is financially supported by JSPS-KAKENHI (JP24H02232, 23K13621, and 22K14591) and JST-CREST (JPMJCR2102).

[1] A. F. Kockum, A. Miranowicz, S. De Liberato, S. Savasta, and F. Nori, Ultrastrong coupling between light and matter, Nat. Rev. Phys. **1**, 19 (2019).

[2] P. Forn-Díaz, L. Lamata, E. Rico, J. Kono, and E. Solano, Ultrastrong coupling regimes of light-matter interaction, Rev. Mod. Phys. **91**, 025005 (2019).

[3] Y. Li, W. Zhang, V. Tyberkevych, W.-K. Kwok, A. Hoffmann, and V. Novosad, Hybrid magnonics: Physics, circuits, and applications for coherent information processing, J. Appl. Phys. **128**, 130902 (2020).

[4] M. Harder, B. M. Yao, Y. S. Gui, and C.-M. Hu, Coherent and dissipative cavity magnonics, J. Appl. Phys. **129**, 201101 (2021).

[5] D. Lachance-Quirion, Y. Tabuchi, A. Gloppe, K. Usami, and Y. Nakamura, Hybrid quantum systems based on magnonics, Appl. Phys. Exp. **12**, 070101 (2019).

[6] G. Bourcin, J. Bourhill, V. Vlaminck, and V. Castel, Strong to ultrastrong coherent coupling measurements in a YIG/cavity system at room temperature, Phys. Rev. B **107**, 214423 (2023).
[7] I. Golovchanskiy, N. N. Abramov, V. S. Stolyarov, A. A. Golubov, M. Yu. Kupriyanov, V. V. Ryazanov, and A. V. Ustinov, Approaching deep-strong on-chip photon-to-magnon coupling, Phys. Rev. Appl. **16**, 034029 (2021).
[8] I. A. Golovchanskiy, N. N. Abramov, V. S. Stolyarov, M. Weides, V. V. Ryazanov, A. A. Golubov, A. V. Ustinov, and M. Y. Kupriyanov, Ultrastrong photon-to-magnon coupling in multilayered heterostructures involving superconducting coherence via ferromagnetic layers, Sci. Adv. **7**, eabe8638 (2021).
[9] A. Ghirri, C. Bonizzoni, M. Maksutoglu, A. Mercurio, O. Di Stefano, S. Savasta, and M. Affronte, Ultrastrong magnon-photon coupling achieved by magnetic films in contact with superconducting resonators, Phys. Rev. Appl. **20**, 024039 (2023).
[10] M. Harder and C.-M. Hu, Chapter two - Cavity spintronics: An early review of recent progress in the study of magnon–photon level repulsion, Solid State Phys. **69**, 47 (2018).
[11] M. Harder, Y. Yang, B. M. Yao, C. H. Yu, J. W. Rao, Y. S. Gui, R. L. Stamps, and C. M. Hu, Level attraction due to dissipative magnon-photon coupling, Phys. Rev. Lett. **121**, 137203 (2018).
[12] X. Zhang, A. Galda, X. Han, D. Jin, and V. M. Vinokur, Broadband nonreciprocity enabled by strong coupling of magnons and microwave photons, Phys. Rev. Appl. **13**, 044039 (2020).
[13] L. D. Barron and J. Vrbancich, Magneto-chiral birefringence and dichroism, Mol. Phys. **51**, 715 (1984).
[14] G. L. J. A. Rikken and E. Raupach, Observation of magneto-chiral dichroism, Nature **390**, 493 (1997).
[15] M. Vallet, R. Ghosh, A. Le Floch, T. Ruchon, F. Bretenaker, and J.-Y. Thépot, Observation of magnetochiral birefringence, Phys. Rev. Lett. **87**, 183003 (2001).
[16] Y. Okamura, F. Kagawa, S. Seki, M. Kubota, M. Kawasaki, and Y. Tokura, Microwave magnetochiral dichroism in the chiral-lattice magnet Cu_2OSeO_3, Phys. Rev. Lett. **114**, 197202 (2015).
[17] S. Tomita, K. Sawada, A. Porokhnyuk, and T. Ueda, Direct Observation of magnetochiral effects through a single metamolecule in microwave regions, Phys. Rev. Lett. **113**, 235501 (2014).
[18] S. Tomita, H. Kurosawa, K. Sawada, and T. Ueda, Enhanced magnetochiral effects at microwave frequencies by a single metamolecule, Phys. Rev. B **95**, 085402 (2017).
[19] S. Tomita, H. Kurosawa, T. Ueda, and K. Sawada, Metamaterials with magnetism and chirality, J. Phys. D: Appl. Phys. **51**, 083001 (2018).
[20] Y. Tokura and N. Nagaosa, Nonreciprocal responses from non-centrosymmetric quantum materials, Nat. Commun. **9**, 3740 (2018).
[21] S. Toyoda, N. Abe, and T. Arima, Nonreciprocal refraction of light in a magnetoelectric material, Phys. Rev. Lett. **123**, 077401 (2019).
[22] See Supplemental Material at http://link.aps.org/supplemental/10.1103/PhysRevApplied.23.L011004 for ac magnetic and electric fields in the waveguide, numerical simulation and theoretical consideration details, the chiral resonant photon modes, measured and simulated spectra without dc magnetic fields, measured spectra of the *z*-axis-oriented metamolecule, measured nonreciprocal spectra, comparison with previous studies, and simulated spectra in free-space.
[23] T. Ueda and M. Tsutsumi, Left-handed transmission characteristics of ferrite microstrip lines without series capacitive loading, IEICE Trans. Electron. **E89-C**, 1318 (2006).
[24] T. Kodama, Y. Kusanagi, S. Okamoto, N. Kikuchi, O. Kitakami, S. Tomita, N. Hosoito, and H. Yanagi, Microwave spectroscopy of a single Permalloy chiral metamolecule on a coplanar waveguide, Phys. Rev. Appl. **9**, 054025 (2018).
[25] D. M. Pozar, *Microwave Engineering 3rd. Edition* (John Wiley & Sons, New York, 2005).
[26] Y. Cao, P. Yan, H. Huebl, S. T. B. Goennenwein, and G. E. W. Bauer, Exchange magnon-polaritons in microwave cavities, Phys. Rev. B **91**, 094423 (2015).
[27] X. Zhang, C-L. Zou, L. Jiang, and H. X. Tang, Strongly coupled magnons and cavity microwave photons, Phys. Rev. Lett. **113**, 156401 (2014).
[28] L. Bai, M. Harder, Y. P. Chen, X. Fan, J. Q. Xiao, and C.-M. Hu, Spin pumping in electrodynamically coupled magnon-photon systems, Phys. Rev. Lett. **114**, 227201 (2015).
[29] T. Chiba, T. Komine, and T. Aono, Microwave transmission theory for on-chip ultrastrong-coupled magnon-polariton in dynamical inductors, J. Mag. Soc. Jpn. **48**, 21 (2024).
[30] X. Li, M. Bamba, Q. Zhang, S. Fallahi, G. C. Gardner, W. Gao, M. Lou, K. Yoshioka, M. J. Manfra, and J. Kono, Vacuum Bloch–Siegert shift in Landau polaritons with ultra-high cooperativity, Nat. Photonics **12**, 324 (2018).
[31] K. Hayashida, T. Makihara, N. Marquez Peraca, D. Fallas Padilla, H. Pu, J. Kono, and M. Bamba, Perfect intrinsic squeezing at the superradiant phase transition critical point, Sci. Rep. **13**, 2526 (2023).
[32] A. Bayer, M. Pozimski, S. Schambeck, D. Schuh, R. Huber, D. Bougeard, and C. Lange, Terahertz light–matter interaction beyond unity coupling strength, Nano Lett. **17**, 6340 (2017).
[33] S. Rajabali, S. Markmann, E. Jöchl, M. Beck, C. A. Lehner, W. Wegscheider, J. Faist, and G. Scalari, An ultrastrongly coupled single terahertz meta-atom, Nat. Commun. **13**, 2528 (2022).
[34] J. A. Kong, *Electromagnetic Wave Theory* (EMW Publishing, Cambridge, 2005).
[35] V. S. Asadchy, A. Díaz-Rubio, and S. A. Tretyakov, Bianisotropic metasurfaces: Physics and applications, Nanophotonics **7**, 1069 (2018).
[36] T. Kodama, T. Nakanishi, K. Sawada, and S. Tomita, Pure moving optical media consisting of magnetochiral metasurfaces, Opt. Mater. Exp. **14**, 2499 (2024).
[37] K. Sawada and N. Nagaosa, Optical magnetoelectric effect in multiferroic materials: Evidence for a lorentz force acting on a ray of light, Phys. Rev. Lett. **95**, 237402 (2005).